 doi:10.20944/preprints202210.0066.v1

*Review*

# A Structure-based View on ABC-transporter linked to Multi-drug Resistance

**Jiahui Huang [1], Gerhard F. Ecker [1,*]**

[1] Department of Pharmaceutical Sciences, University of Vienna, Vienna, Austria
* Correspondence: gerhard.f.ecker@univie.ac.at

**Abstract:** The discovery of first ATP-binding cassette (ABC) transporter, whose overexpression in cancer cells is responsible for exporting anticancer drugs out of tumor cells, initiated enormous efforts to overcome tumor cell multidrug resistance (MDR) by inhibition of ABC-transporter. Because of its many physiological functions, diverse studies have been conducted on the mechanism, function and regulation of this important group of transmembrane transport proteins. In this review, we will focus on the structural aspects of this transporter superfamily. Since the resolution revolution of electron microscope, experimentally solved structures increased rapidly. A summary of the structures available and an overview of recent structure-based studies are provided. More specifically, the artificial intelligence (AI)-based predictions from AlphaFold 2 will be discussed.

**Keywords:** structure-based studies; ABC transporter; multidrug resistance (MDR); cancer therapy

## 1. Introduction

Cancer is the second leading cause of mortality in the European Union after cardiovascular diseases, 2020 alone, about 2.7 million people in the 27 EU countries were diagnosed with cancer, and nearly 1.3 million die from it [1]. Though large effort was made on cancer therapy, lives lost to cancer in the EU still tend to increase [2]. A major obstacle in cancer treatment is the development of resistance to many structurally dissimilar cytotoxic substances. This phenomenon is termed as multidrug resistance (MDR), which causes the cancer cell ineffectiveness in accumulating drugs, related to activity of an energy-dependent unidirectional, membrane-bound, drug-efflux transporter proteins. They belong to the ATP-binding cassette (ABC) transporter superfamily. In total, the human ABCome is composed of 48 genes, which encodes seven subfamilies of ABC transporter proteins on the premise of sequence divergence and structural arrangement. The following nomenclature (alternative symbol in parenthesis) was suggested by the Human Genome Organization's Gene Nomenclature Committee (HGNC): ABCA(ABC1), ABCB(MDR), ABCC(MRP/CFTR), ABCD(ALD), ABCE(OABP), ABCF(GCN20) and ABCG(WHITE).

The first human ABC transporter, P-glycoprotein (P-gp, encoded by the MDR-1/ABCB1 gene), was characterized in 1976 [3]. Subsequent to the discovery of P-gp, studies of cancer cell revealed other phenotypes, which showed multidrug resistance related characteristics. These multidrug resistance related proteins (MRPs) were later classified as the ABCC subfamily [4]. Simultaneously, a novel half transporter member of the ABC superfamily was identified from a resistant breast cancer cell line [5], hence named as breast cancer resistance protein (BCRP, encoded by the ABCG2 gene). Of all 48 human ABC transporters that have been described so far, these three aforementioned members are predominantly linked to MDR.

In principle, an ABC transporter comprises four domains, namely two transmembrane domains (TMDs) embedded in the lipid bilayer, and two nucleotide binding domains (NBDs) facing the cytoplasmatic space. The human ABC transporters can be either full- or half-transporters. In the full transporter transcript, the motifs are arranged as N-

 doi:10.20944/preprints202210.0066.v1

TM-NB-TM-NB-C, whereas the latter ones have only one TM and one NB. Hence the half-transporters should form homodimers or heterodimers to perform the function. The typical TMDs are consist of 2 × 6 $\alpha$-helices, which construct together one centralized efflux path for a variety of substrates. This folding pattern is conserved among the eukaryotic cells with, however, a lower sequence conservation comparing to the NBDs [6,7]. In the NBDs, where binding and hydrolysis of ATP takes place, some motifs are highly conserved, such as Walker-A, Walker-B, signature sequence (also as linker peptide or Walker-C motif) [8], Histidine loop [9], and Glutamine loop [10].

With enhanced direct electron detectors [11] and image-processing packages [12], cryo-electron microscopy (cryo-EM) has elevated the progress of structural biology. This short review mainly focuses on those three ABC transporter members (ABCB1, ABCC1 and ABCG2), which are predominantly linked to the phenomenon of MDR [13]. We summarize the research state from the structural biology aspect as well as structure-based in-silico analyses. Finally, the impact of AlphaFold is discussed.

## 2. ABCB1

P-glycoprotein (P-gp, P for permeability), by far the best-known and well-studied ABC-transporter, is composed of 1280 amino acids (170 kDa). In 2018, Kim et al. published for the first time a cryo-EM structure of human ABCB1 in an ATP-bound, outward-facing conformation, at a resolution of 3.4 Å (PDB code: 6C0V) [14]. Subsequently, Alam et al. Obtained series of three-dimensional (3D) structures of human P-gp via cryo-EM in a nucleotide-free state (PDB code: 6QEX, 6FN4, 6FN1) with resolution from 3.58 to 4.14 Å. Remarkedly, they managed to solve the structures both in substrate (Taxol: a chemotherapeutic compound) and inhibitor-bound (Zosuquidar: a third generation ABCB1 inhibitor) states. These inward-open and occluded conformations demonstrate the plasticity of the central binding pocket in the way how the side chains and backbone rearrange [15]. More refined structures were reported by Nosol et al. in complex with the Fab fragment of an inhibitory monoclonal antibody MRK16 [16]. The highest resolution (3.2 Å) among their retrieved structures is with vincristine (an antitumor drug) in a substrate-bound occluded state (PDB code: 7A69). Besides capturing another conformation of the substrate binding modus, they also determined additional structures (PDB code: 7A6C, 7A6E) bound with other potent inhibitors (elacridar and tariquidar).

As known that P-gp has a broad spectrum of substrate, this wide substrate specificity also refers to a crucial obstacle of designing specific ABCB1 inhibitors. Unspecific inhibitors (like vanadate), which target the conserved ATPase sites, is out of scope from this review. Instead, specific inhibitors, that compete with substrates for binding, is the point of discussion. Both Alam and Nosol observed a single substrate transporting, but an in-pair inhibitors interaction in the same drug binding pocket. Moreover, there were existing report about potential transporting process for inhibitors (elacridar and tariquidar) under a very low concentration [17]. These observations suggest that there is no strict boundary between substrates and inhibitors, but to which extent the small molecule occupies and interacts with the central cavity or even beyond [16]. In general, it is worth noticing that the central binding site of human ABCB1 is mainly composed of aromatic side chains. In addition, the cytoplasmatic gate region (also being called access tunnel) participating in inhibitor binding is relative acidic. These observations are consistent with the fact that P-gp moderators are generally hydrophobic, positive charged or neutral.

## 3. ABCC1

When analyzing P-gp expression in different tumor types it turned out that some cell lines process a high level of drug efflux but do not show upregulation of P-gp expression. In 1992, Cole et al. managed to clone a cDNA encoding a specific transporter protein of 170kDa, and termed it multidrug resistance related protein 1 (MRP1) [4]. Later, it was grouped into the C-subfamily of ABC transporter through sequence analysis. According to HUGO Human Gene Nomenclature, the C-class human ABC protein gene family

 doi:10.20944/preprints202210.0066.v1

includes 12 members. Among them, nine are multidrug resistance related, namely MRP1-9 (or ABC1-6, ABC10-12). Besides that, there is also the cystic fibrosis transmembrane conductance regulator (CFTR/ABCC7), which is an ATP-gated chloride channel instead of an active transporter [18]. The other two are sulfonylurea receptors SUR1 and SUR2 (or ABCC8, ABCC9 respectively), known as a component of an ATP sensitive potassium channel [19].

Topologically, the C-subfamily can be divided into "long" and "short" proteins. In general, the structural pattern of a typical ABC transporter remains, namely two TMDs and two NBDs. The only difference between the "long" and "short" ABCC proteins is an extra transmembrane domain 0 (TMD0, approximately 250 amino acids in addition) on the N-terminal of the long ones. This additional domain exists in 5 MRP members, namely MRP1, MRP2, MRP3, MRP6, MRP7 (ABCC1/2/3/6 and ABCC10 respectively), as well as in SUR1, SUR2 [20]. Interestingly, this TMD0 was reported as an influence but not essential for the transport function of ABCC1. Leukotriene C4 (LTC4, an endogenous substrate of MRP1 [21,22]) can still be transported without this domain [23], whereas certain mutations on it can reduce the transport activity [24,25]. Moreover, the loop 0 (L0) connecting TMD0 with TMD1, also called lasso motif in other MRPs [26] , has been shown to engaged in intracellular recycling process [27] and transport activity [23], being probably even engaged in the gating process [28] of the two NBDs during catalytic process.

At present, MRP1 is the first and best-studied ABCC/MRP protein in the field of clinical oncology [29]. Unfortunately, after almost 30 years since the discovery of ABCC1, the exact 3D structure of the human ABCC1 has not been successfully determined yet. Alternatively, other eukaryotic molecular structures are available: they are from Bos taurus and were published by the same research group from the year 2017 to 2020 (PDB code: 6UY0, 6BHU, 5UJ9, 5UJA) [30-32]. The bovine MRP1 (bMRP1) is close to the human transporter (hMRP1) both in sequence similarity (91%), and substrate affinity [29,33,34]. Based on this fact, analyzing the available bovine structures in different conformations (inward-facing, substrate-bound, outward-facing) can help to gain insights of hMRP1 structural determinants for substrate recognition and transport. Like P-gp, MRP1 is also capable of recognizing a diversity of structurally unrelated molecules, however, through totally different mechanism. The substrate-binding site of MRP1 is rather small and bipartite, composed of a positively charged and a hydrophobic region [33]. A ramification of this fact is that the whole transporting pathway of MRP1 is basic, which explains its trafficking preference of organic acids with large hydrophobic groups [35].

**4. ABCG2**

Subsequent to the discovery of ABCC1, three different research groups independently found another multidrug efflux transporter. Originally it was named as breast cancer resistance protein (BCRP [5]), ABC transporter overexpressed in placenta (ABCP [36]), or mitoxantrone resistance (MXR [37]) protein, respectively. Based on sequence similarity and structural organization [38], it was assigned to the ABCG subfamily. The human G-class ABC protein subfamily is composed of six half transporters arranged as N-NB-TM-C, which is opposite to the other ABCs (TM at the N-terminus). Among them, the second member ABCG2 is the one which confers resistance to several anticancer drugs [39,40].

ABCG2 is a membrane protein consisting of 655 amino acids (72 kDa). Its functional unit is minimal a homodimer, although reports about higher order homo-oligomers also have been published [41-43]. Nevertheless, high-resolution structures of human ABCG2 thus far are all determined as dimer [44-49]. As a half transporter with shorter sequence, ABCG2 differs to the other two aforementioned human multidrug transporters ABCB1 and ABCC1 with respect to domain-swapping and TM-extension into cytosol. Consequently, it has a unique substrate capture and transport mechanism. The first experimental solved full human ABCG2 occluded structure by Jackson et al. [45] in 2018 confirmed the intriguing finding of Taylor et al. [44] in 2017. They demonstrate an adjacent

Preprints (www.preprints.org) | NOT PEER-REVIEWED | Posted: 6 October 2022 doi:10.20944/preprints202210.0066.v1

architecture of the NBDs under the inward facing occluded status, while the NBDs of the full transporters stay separated under this conformational state. Orlando et al. [47] from the same group managed in 2020 to capture the resting ABCG2 in an antibody-, substrate- and inhibitor-free condition. The resting ABCG2 stabilizes in an inward facing apo conformation with the TMDs being separated as in the inward facing occluded conformation, but the TM5s shift towards the dimer axis to seal off the crevice in absence of bound inhibitor/substrate (Figure 1a). In comparison to that, both TMDs and NBDs of ABCB1 and ABCC1 adopt an open conformation to the cytoplasmatic side in the apo state (Figure 1b, 1c).

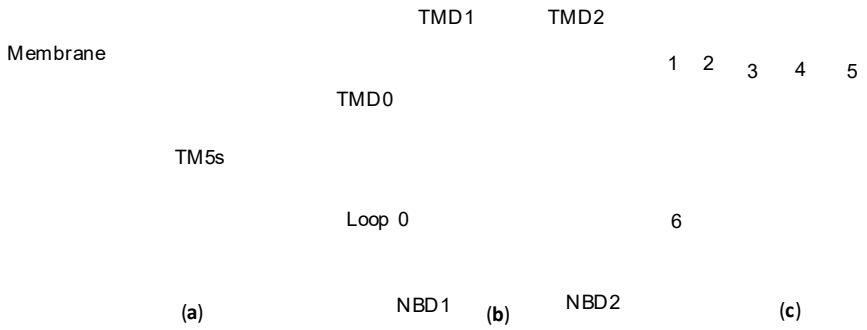


**Figure 1.** Inward facing apo conformation comparison of ABCG2 dimer (one monomer in orange, another in yellow) with ABCB1 and ABCC1. (a) Two TM5s from two ABCG2 subunits rotate towards the central crevice, while the rest TMs of the NBD rotate towards the intracellular space. (b) ABCB1 and ABCC1 are full transporter with two TMDs and NBDs (TMD1 and NBD1 in blue, TMD2 and NBD2 in green), while the ABC1 comprises an extra TMD0 colored in grey connected by loop 0. (c) Topology diagram of P-gp TMD1 colored in blue with two helixes (TM4 and TM5) cross-over the central axis.

Overall, the group of Kaspar P. Locher has been publishing a variety of human ABCG2 structure through cryo-EM since 2017. Various conformational states were captured (Table 1), including inward-facing (IF) apo (PDB: 5NJ3, 5NJG), inward-facing inhibitor/substate bound (PDB: 6FFC, 6ETI, 6FEQ, 6HIJ, 6HCO, 6VXH, 6VXI, 6VXJ), apo closed (PDB: 6VXF), and outward facing (OF) ATP bound states (PDB: 6HBU, 6HZM). Although both substrates and inhibitors from all occluded structures were determined in a predominantly overlapped cavity center, they perform different dynamics moderation upon the transporter activity. As substrates, estrone-3-sulphare (E1S) or mitoxantrone (MXN) or 7-Ethyl-10-hydroxycamptothecin (SN38), were found as a single molecule in the binding site and can be translocated to extracellular space. However, two molecules of inhibitor MZ29 (a derivative of fungal toxin fumitremorgin [50], selective inhibitor of ABCG2 with neurotoxicity) occupied the same pocket, but reach out approaching the cytoplasmic membrane boundary to establish enhanced interactions. Meanwhile, it shapes a larger density than partial inhibitor MB136 (a derivative of tariquidar [51], a third-generation ABCB1 inhibitor), and imatinib [52-54], which can fit only one molecule into that cavity. Yet, contact strength and molecular volume are not the only fact that differentiate an inhibitor from a substrate. As a mutagenesis study (on Arg482 [55]) outside the known binding site can totally reverse the inhibition. Nevertheless, the known binding modes of substrates and (partial) inhibitors can still serve as a boundary example for the future design of ABCG2 moderators.

Preprints (www.preprints.org) | NOT PEER-REVIEWED | Posted: 6 October 2022 doi:10.20944/preprints202210.0066.v1

**Table 1.** Summary of cryo-EM structures of human ABCG2

| PDB | Conformation | Cocrystal-molecules | Property | Resolution (Å) | References |
|---|---|---|---|---|---|
| 5NJ3 | IF (NBDs modeled) | - | - | 3.78 | Taylor et al. 2017[44] |
| 5NJG | IF (Only TMDs) | - | - | 3.78 | Taylor et al. 2017[44] |
| 6FFC | IF | MZ29*2 | Inhibitor | 3.56 | Jackson et al. 2018[45] |
| 6ETI | IF | MZ29*2 (Fab) | Inhibitor | 3.10 | Jackson et al. 2018[45] |
| 6FEQ | IF | MB136 (Fab) | Inhibitor | 3.6 | Jackson et al. 2018[45] |
| 6HIJ | IF | MZ29*2 (Cholesterol and phospho-lipid surrounded) | Inhibitor | 3.56 | Jackson et al. 2018[45] |
| 6HCO | IF | E1S | Substrate | 3.58 | Manolaridis et al. 2018[46] |
| 6HZM | OF | ATP*2+Mg2+ (Alternative placement) | - | 3.09 | Manolaridis et al. 2018[46] |
| 6HBU | OF | ATP*2+Mg2+ | - | 3.09 | Manolaridis et al. 2018[46] |
| 6VXF | Apo-closed | - | - | 3.50 | Orlando et al. 2020[47] |
| 6VXH | IF | Imatinib | Inhibitor | 4.00 | Orlando et al. 2020[47] |
| 6VXI | IF | Mitoxantrone | Substrate | 3.70 | Orlando et al. 2020[47] |
| 6VXJ | IF | SN38 | Substrate | 4.10 | Orlando et al. 2020[47] |

**5. Protein Models and AlphaFold 2**

Despite decades of investment from structural biologists, till now less than 10% of the human proteins have experimentally solved 3D coordinates deposited in the Protein Data Bank (PDB). (Protein-level coverage), which corresponds to approximately 17% of the sequence in the human proteome (residue-level coverage) [56]. However, this number could be considerably enhanced by creating protein homology models based on template structures from other species. When analyzing the structural landscape of ABC-transporter: we retrieved 160 available experimental solved human structures from PDB covering 24 ABC-transporter members. for all ABC-transporters protein models can be found in SWISS-MODEL repository. Under circumstances, when no decent structure/model is available, all ABC transporters have suitable templates in PDB for modeling with higher than 70% sequence similarity.

Briefly, this analysis is based on a KNIME [57] workflow which summaries the up-to-date status of the structural feasibility of all 48 ABC-transporter subfamilies. Upon a list of PDB identifier and entity ID, other experimental information, for instance method, resolution, sequence coverage, co-crystallized small molecules, and release data, are also simultaneously extracted by the workflow. If extra requirement appears, a threshold can be addressed on any aforementioned parameters. For instance, a 75% sequence coverage cut-off for the experimental solved structure comparing to full canonical sequence would filter out 59 structures and 3 transporter members, in which 91 are protein-ligand complexes (Figure 2a). Plotting structure resolution value with the releasing time or ABC gen name reveals that fact: 1) More than half of the structures (94 out of 160) were solved in

Preprints (www.preprints.org) | NOT PEER-REVIEWED | Posted: 6 October 2022 doi:10.20944/preprints202210.0066.v1

last three years (Figure 3). 2) Experimental solved structure with lower than 3.5 Å resolution takes 62% (99 out of 160) included both X-ray and cryo-EM solved structures of all concatenates (Figure 2b).

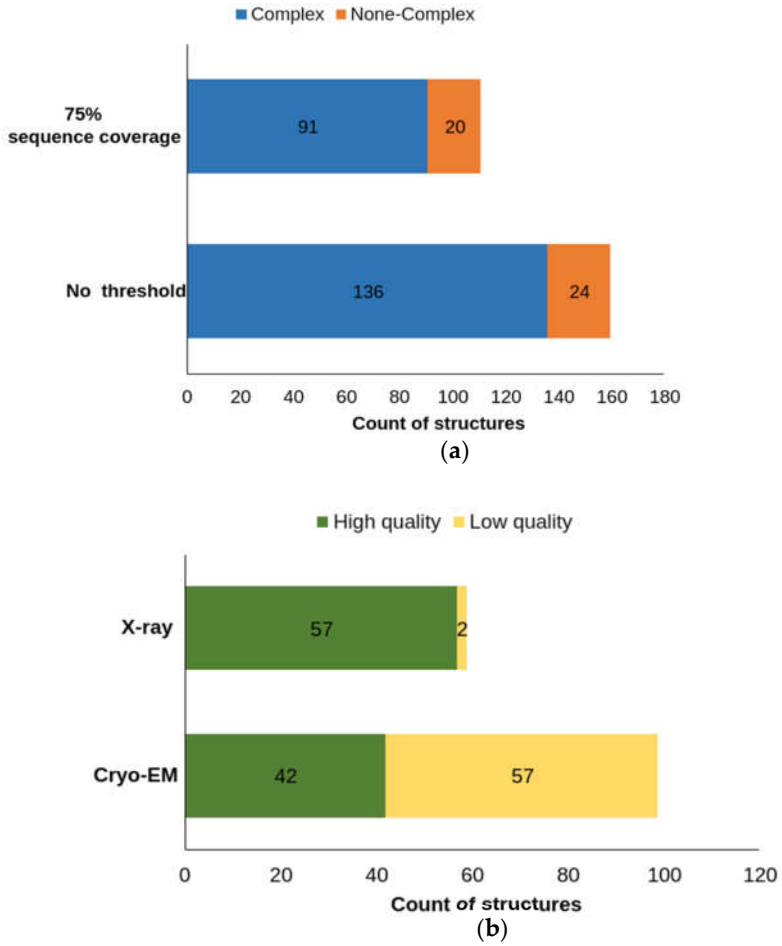


**Figure 2.** Composition of PDB structure. Blue fraction is the structures with co-crystalized small molecules, and the orange part is the ones without. (a) Totally, 160 PDB structures are retrieved for all 48 ABC-transporters, in which 136 concatenates contain crystalized small molecules. A threshold of 75% sequence coverage filters out 59 structures, leaving 101 experimental solved human ABC structures. Among which 20 are none-complex, 91 are protein-compound complex. (b) For the total 160 PDB structures, 99 structure possess a resolution value lower than 3.5 Å, among which 42 are solved by X-ray, 57 are from cryo-EM. Apart from these two methods, one structure was found solved by NMR, which is not included in bar chart.

Preprints (www.preprints.org) | NOT PEER-REVIEWED | Posted: 6 October 2022 doi:10.20944/preprints202210.0066.v1

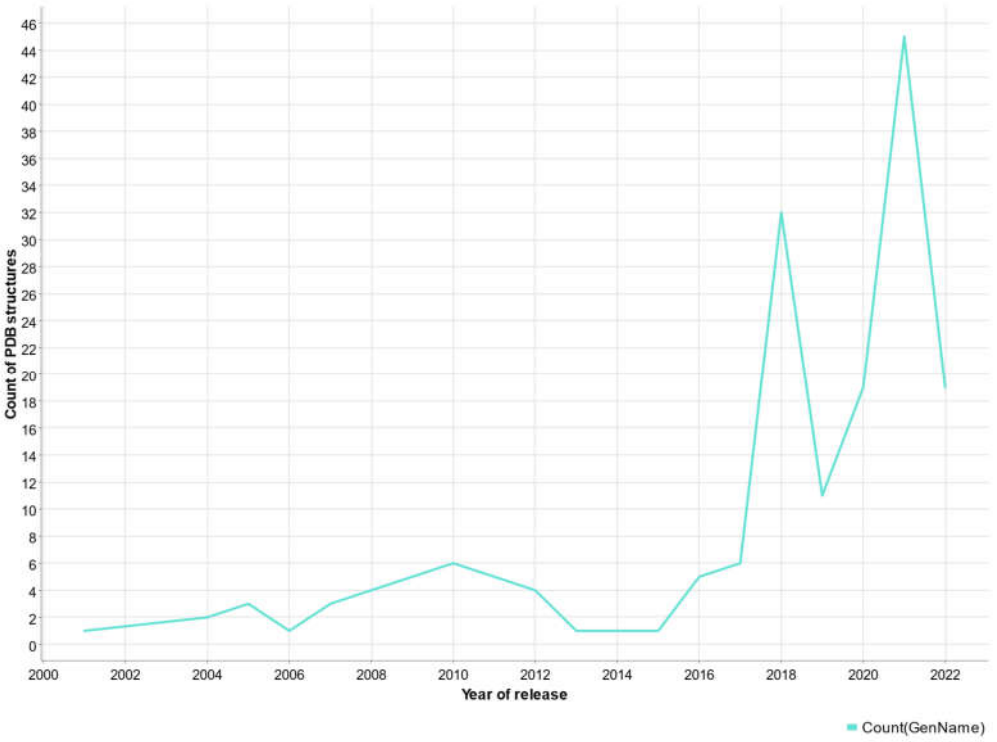


**Figure 3.** Plot of experimental solved structures number to time of the releasement.

Finally, the availability of AlphaFold 2, an artificial intelligence approach for protein 3D structure prediction based on a neural network [58] had huge impact on the field. In the AlphaFold 2 database (https://www.alphafold.ebi.ac.uk/download), 98.5% of all human proteins have a structural prediction. Therein, 58% of all modelled residues have a high (>70) confidence score (pLDDT, predicted local distance difference test score). This score scales between 0 to 100, in which a larger number indicates higher confidence on the prediction.

Taking example of human ABCB1, despite the significant success in solving the overall structure, the communication between NBD and TMD remains unknown. The region between Ala631 and Pro693 connecting NBD1 with TMD2 is absent in all experimental determined structures but present in the AlphaFold prediction. It is known as a flexible linker being involved in substrate specificity and conformational change completing the full transport circle [59,60] The group of dos Santos has been studying this region intensively via docking, homology modelling and molecular dynamics [61,62]. Their latest update [63] on the linker secondary structure demonstrates a different configuration (available under this link: http://chemistrybits.com/downloads/systems/) as it is presented in the AlphaFold 2 database, while both are in an inward-facing conformation. When superposed in Molecular Operation Environment (MOE) (Chemical Computing Group, 2019 software suite) [64], AlphaFold prediction shows a higher expose level with the upper loop extending into the cytoplasmatic space, along with an extra helix segment on the lower part (Figure 4a). Whereas, the finalized model from dos Santos suggests a larger protein-protein contact surface with a more compact coil (Figure 4b).

Indeed, this linker domain is a highly flexible region. Along the years, models published by the dos Santos group have also been adjusting with the availability of murine and human P-gp crystal structures. Such intrinsically disordered regions (IDRs) are often depicted as very low confidence (pLDDT<50) region in AlphaFold predictions. Regions with very low pLDDT score are suggested by Ruff et al. [65] no to be interpreted as structure but rather as a prediction of disorder.

Preprints (www.preprints.org) | NOT PEER-REVIEWED | Posted: 6 October 2022 doi:10.20944/preprints202210.0066.v1

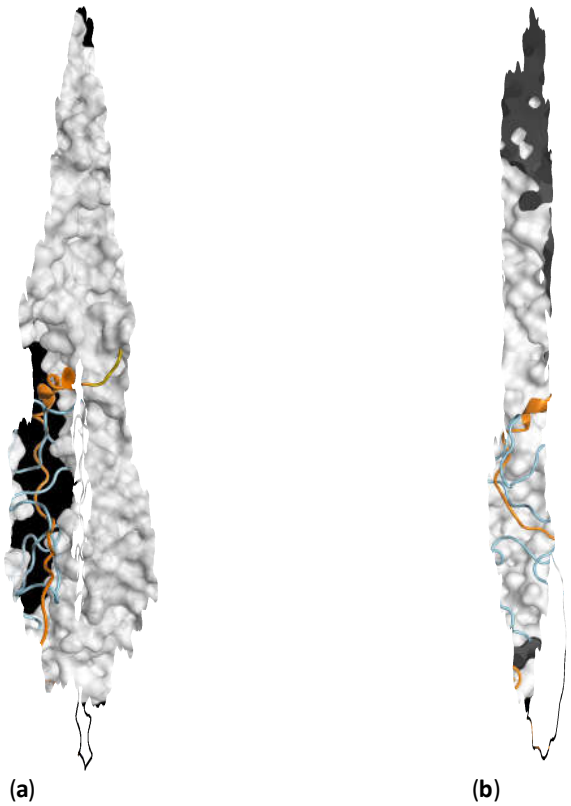


**Figure 4.** Flexible linker configuration between NBD1 and TMD2 of P-gp. Linker of AlphaFold 2 prediction colored in orange, indicating a low confidence pLDDT value. In comparison to AlphaFold position, model from dos Santos group packs the linker in blue tighter in the crevice. (a) Linker position in the interface of P-gp (linker from AlphaFold model in orange, linker from dos Santos group in blue). (b) The folding the link viewing from the view of the interface.

Aside from the disordered region, defined secondary structures can be determined heterogeneous between experimental solved structures and AlphaFold 2 DB model prediction. As an example, TMD0 structures of bMPR1 published by Johnson et al. [30] and Chen et al. [31] from 2017 to 2018 are up-to-now the only experimental determined results. This is yet absent in the new bMPR1 cryo-EM structure released by Wang et al. together with Johnson and Chen in 2020 [32]. The conformational transition cross transport cycle is shown to be mainly conducted by the TMDs and the NBDs, while the TMD0 undergoing a minor adjustment (Figure 5b). In comparison, TMD0 in the model from AlphaFold 2 derivates another conformation leaning closer to the TMD1, though the rest of the structure superposes well with the inward-facing ligand bound structure (Figure 5a). The majority of the TMDs of AlphaFold model are predicted with high confidence value (pLDDT score > 70), yet the discrepancy of the TMD0 determination is unneglectable.

Noteworthy, the local resolution (5 Å) of TMD0 in the first bMRP1 structure is reported as far from satisfactory [30]. The electro-density correspond to this region is present but insufficient for connectivity and residues detail assignment for every structure published thus far. Eventually, all available TMD0 region are polyalanine models fitting to stereochemistry statistics and overall geometry of the cryo-EM map with the highly flexible loop 0 (L0) connecting TMD0 and TMD1. This leads to an ambiguous discrimination referring to the conformational variation of TMD0 in AlphaFold 2 model.

Preprints (www.preprints.org) | NOT PEER-REVIEWED | Posted: 6 October 2022 doi:10.20944/preprints202210.0066.v1

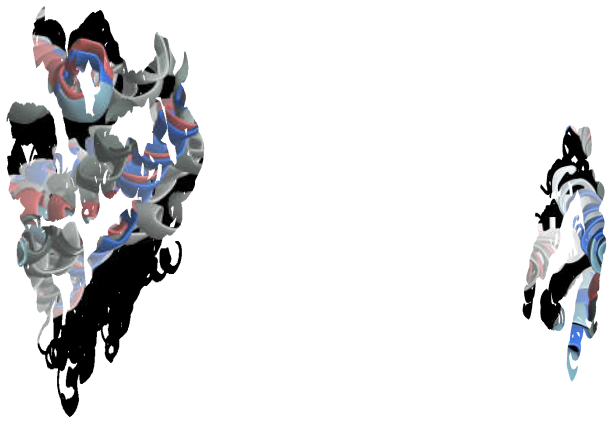


**Figure 5.** Conformational arrangement bMRP1 viewing from intracellular side in MOE. (a) Superposition of the cryo-EM structures in different conformational states (Pink: inward-facing apo, 5UJ9; light grey: inward-facing occluded, 5UJA; dark grey: outward-facing ATP-bound, 6BHU). Together with AlphaFold 2 prediction colored according to the pLDDT value scale (Dark blue: pLDDT>90, light blue: 90>pLDDT>70, yellow: 70>pLDDT>50, orange: 50>pLDDT). (b) Under this superposition, TMD0 of AlphaFold model undergoing another conformational derivation while the rest of the TMDs align well with TMDs of the cryo-EM inward-facing structure in pink.

The advantage of AlphaFold generating non-template-based full chain prediction, however, becomes a limitation in the case of polypeptide chain. As a half-transporter, only a monomer is presented in the AlphaFold database. A widely accepted concept of ABCG2 functional unit is as a homodimer [66,67], while other higher order oligomers are suggested to serve as regulators for the dimeric form [68]. Without a decent arrangement of the subunits, the value of the structural model is limited. On one hand, intermolecular interaction between two halves can only be accessed in classical template-based homology models [69] before crystal structure was solved in 2017. Although, it was proven later that those intermolecular disulfide bridges are not essential for the activity [70], and they might result from oxidation processes during sample preparation [68]. On the other hand, the central cavity for ligand as well as inhibitor binding can only be accessed in the dimeric form. It was observed in multiple cryo-EM structures, that substrates [46,48] (like estrone-3-sulphate, cholesterol, mitoxantrone, topotecan, tariquidar) and inhibitors [45] (Ko143, MZ29, and tariquidar-derivatives like MB136) bind in the same pocket on the symmetry axis. While inhibitors extend over the critical accommodate volume, and establish extra interaction beyond, they seal the transporter in an inward facing conformation. With one monomer structure from AlphaFold prediction, neither the intermolecular interaction nor the binding pocket composition can be reached. Moreover, conformational transformation during transport circle requires also the full functional formation.

Eventually, AlphaFold 2 is not the main focus of this review. Besides, DeepMind released also the whole algorithm framework of AlphaFold2 in GitHub [58] with which one can further explore other possibility, such as generating structural predictions in multiple conformations, as well as new folding patterns. Above all, the novel deep learning framework developed by DeepMind has still the potential to reverse-feed structural biology by providing predicted model fitting into cryo-EM density [71] or by molecular replacement to solve X-Ray structure [72]. Hence, it should accelerate the determination process the human ABCC1 structure. Even when experimental determined structure is available, like

 doi:10.20944/preprints202210.0066.v1

ABCB1 and ABCG2, computational prediction can still provide valuable information, such as signaling die disorder level of a region, or presenting the structure in another conformation.

## 6. Conclusion

Reversing MDR remains a major challenge in cancer chemotherapy. Aforementioned ABC transporter members are the most studied targets towards unraveling the mechanism of drug resistance in cancer therapy. In the past decades, the research on these proteins was enormously hampered by the fact that membrane proteins are extremely troublesome to extract and purify. However, considerable progress was made by the structural biologists. This comprises not only solving 3D coordinate experimentally, but also generating reliable predictions. Two out of these three aforementioned human ABC transporters have multiple cryo-EM structures along the transition time line. Only ABCC1 has no experimental solved structure so far, but the bovine homologues with sequence similarity higher than 90% served as valuable templates for protein homology models of the human analog. In addition, AlphaFold 2 predictions can serve as a powerful source for 3D protein models.

**Supplementary Materials:** Not applicable.

**Author Contributions:** Conceptualization, G.E. and J.H.; writing—original draft preparation, J.H.; writing—review and editing, G.E; supervision, G.E. All authors have read and agreed to the published version of the manuscript.

**Funding:** The author has received financial support from the Austrian Science Fund/FWF, grant W1232 (MolTag).

**Institutional Review Board Statement:** Not applicable.

**Informed Consent Statement:** Not applicable.

**Data Availability Statement:** Data is contained within the article or supplementary material.

**Conflicts of Interest:** The authors declare no conflict of interest.

**Sample Availability:** Not applicable.

## Abbreviations

MDR, multidrug resistance; ABC, ATP-binding cassette; HGNC, Human Genome Organization's Gene Nomenclature Committee; P-gp, P-glycoprotein; MRPs, multidrug resistance related proteins; BCRP, breast cancer resistance protein; ABCP, ABC transporter overexpressed in placenta; MXR, mitoxantrone resistance; TMDs, transmembrane domains; NBDs, nucleotide binding domains; cryo-EM, cryo-electron microscopy; LTC4, Leukotriene C4; L0, loop 0; CFTR, cystic fibrosis transmembrane conductance regulator; SUR, sulfonylurea receptors; IF, inward facing; OF, outward facing; pLDDT, predicted local distance difference test score; MOE, molecular operating environment; IDRs, intrinsically disordered regions

## References

1. ECIS – European Cancer Information System. Series of Cancer Factsheets in EU-27 countries. Available online: https://ecis.jrc.ec.europa.eu (accessed on 10 December 2021 ).
2. Ferlay J, L.M., Ervik M, Lam F, Colombet M, Mery L, Piñeros M, Znaor A, Soerjomataram I, Bray F. Global Cancer Observatory: Cancer Tomorrow. Lyon, France: International Agency for Research on Cancer. Available online: https://gco.iarc.fr/tomorrow (accessed on 10 December 2021).
3. Juliano, R.L.; Ling, V. A surface glycoprotein modulating drug permeability in Chinese hamster ovary cell mutants. *Biochimica et Biophysica Acta (BBA)-Biomembranes* **1976**, *455*, 152-162.
4. Cole, S.; Bhardwaj, G.; Gerlach, J.; Mackie, J.; Grant, C.; Almquist, K.; Stewart, A.; Kurz, E.; Duncan, A.; Deeley, R.G. Overexpression of a transporter gene in a multidrug-resistant human lung cancer cell line. *Science* **1992**, *258*, 1650-1654.
5. Doyle, L.A.; Yang, W.; Abruzzo, L.V.; Krogmann, T.; Gao, Y.; Rishi, A.K.; Ross, D.D. A multidrug resistance transporter from human MCF-7 breast cancer cells. *Proceedings of the National Academy of Sciences* **1998**, *95*, 15665-15670.
6. Kerr, I.D. Structure and association of ATP-binding cassette transporter nucleotide-binding domains. *Biochimica et Biophysica Acta (BBA)-Biomembranes* **2002**, *1561*, 47-64.

7. Hanekop, N.; Zaitseva, J.; Jenewein, S.; Holland, I.; Schmitt, L. Molecular insights into the mechanism of ATP-hydrolysis by the NBD of the ABC-transporter HlyB. *FEBS letters* **2006**, *580*, 1036-1041.
8. Walker, J.E.; Saraste, M.; Runswick, M.J.; Gay, N.J. Distantly related sequences in the alpha-and beta-subunits of ATP synthase, myosin, kinases and other ATP-requiring enzymes and a common nucleotide binding fold. *The EMBO journal* **1982**, *1*, 945-951.
9. Linton, K.J.; Higgins, C.F. The Escherichia coli ATP-binding cassette (ABC) proteins. *Molecular microbiology* **1998**, *28*, 5-13.
10. Diederichs, K.; Diez, J.; Greller, G.; Müller, C.; Breed, J.; Schnell, C.; Vonrhein, C.; Boos, W.; Welte, W. Crystal structure of MalK, the ATPase subunit of the trehalose/maltose ABC transporter of the archaeon Thermococcus litoralis. *The EMBO Journal* **2000**, *19*, 5951-5961.
11. McMullan, G.; Faruqi, A.; Henderson, R.; Guerrini, N.; Turchetta, R.; Jacobs, A.; Van Hoften, G. Experimental observation of the improvement in MTF from backthinning a CMOS direct electron detector. *Ultramicroscopy* **2009**, *109*, 1144-1147.
12. Cheng, Y.; Grigorieff, N.; Penczek, P.A.; Walz, T. A primer to single-particle cryo-electron microscopy. *Cell* **2015**, *161*, 438-449.
13. Sharom, F.J. ABC multidrug transporters: structure, function and role in chemoresistance. *Pharmacogenomics* **2008**, *9*, 105-127.
14. Kim, Y.; Chen, J. Molecular structure of human P-glycoprotein in the ATP-bound, outward-facing conformation. *Science* **2018**, *359*, 915-919.
15. Alam, A.; Kowal, J.; Broude, E.; Roninson, I.; Locher, K.P. Structural insight into substrate and inhibitor discrimination by human P-glycoprotein. *Science* **2019**, *363*, 753-756.
16. Nosol, K.; Romane, K.; Irobalieva, R.N.; Alam, A.; Kowal, J.; Fujita, N.; Locher, K.P. Cryo-EM structures reveal distinct mechanisms of inhibition of the human multidrug transporter ABCB1. *Proceedings of the National Academy of Sciences* **2020**, *117*, 26245-26253.
17. Bankstahl, J.P.; Bankstahl, M.; Römermann, K.; Wanek, T.; Stanek, J.; Windhorst, A.D.; Fedrowitz, M.; Erker, T.; Müller, M.; Löscher, W. Tariquidar and elacridar are dose-dependently transported by P-glycoprotein and Bcrp at the blood-brain barrier: a small-animal positron emission tomography and in vitro study. *Drug Metabolism and Disposition* **2013**, *41*, 754-762.
18. Sheppard, D.N.; Welsh, M.J. Structure and function of the CFTR chloride channel. *Physiological reviews* **1999**, *79*, S23-S45.
19. Philipson, L.H.; Steiner, D.F. Pas de deux or more: the sulfonylurea receptor and K+ channels. *Science* **1995**, *268*, 372-374.
20. Chan, K.W.; Zhang, H.; Logothetis, D.E. N-terminal transmembrane domain of the SUR controls trafficking and gating of Kir6 channel subunits. *The EMBO journal* **2003**, *22*, 3833-3843.
21. Leier, I.; Jedlitschky, G.; Buchholz, U.; Cole, S.; Deeley, R.G.; Keppler, D. The MRP gene encodes an ATP-dependent export pump for leukotriene C4 and structurally related conjugates. *Journal of Biological Chemistry* **1994**, *269*, 27807-27810.
22. Müller, M.; Meijer, C.; Zaman, G.; Borst, P.; Scheper, R.J.; Mulder, N.H.; De Vries, E.; Jansen, P. Overexpression of the gene encoding the multidrug resistance-associated protein results in increased ATP-dependent glutathione S-conjugate transport. *Proceedings of the National Academy of Sciences* **1994**, *91*, 13033-13037.
23. Bakos, E.; Evers, R.; Szakács, G.; Tusnády, G.E.; Welker, E.; Szabó, K.; de Haas, M.; van Deemter, L.; Borst, P.; Váradi, A. Functional multidrug resistance protein (MRP1) lacking the N-terminal transmembrane domain. *Journal of Biological Chemistry* **1998**, *273*, 32167-32175.
24. Yang, Y.; Chen, Q.; Zhang, J.-T. Structural and functional consequences of mutating cysteine residues in the amino terminus of human multidrug resistance-associated protein 1. *Journal of Biological Chemistry* **2002**, *277*, 44268-44277.
25. Leslie, E.M.; Bowers, R.J.; Deeley, R.G.; Cole, S.P. Structural requirements for functional interaction of glutathione tripeptide analogs with the human multidrug resistance protein 1 (MRP1). *Journal of Pharmacology and Experimental Therapeutics* **2003**, *304*, 643-653.
26. Zhang, Z.; Chen, J. Atomic structure of the cystic fibrosis transmembrane conductance regulator. *Cell* **2016**, *167*, 1586-1597.
27. Westlake, C.J.; Cole, S.P.; Deeley, R.G. Role of the NH2-terminal membrane spanning domain of multidrug resistance protein 1/ABCC1 in protein processing and trafficking. *Molecular biology of the cell* **2005**, *16*, 2483-2492.
28. Yang, Y.; Liu, Y.; Dong, Z.; Xu, J.; Peng, H.; Liu, Z.; Zhang, J.-T. Regulation of function by dimerization through the amino-terminal membrane-spanning domain of human ABCC1/MRP1. *Journal of Biological Chemistry* **2007**, *282*, 8821-8830.
29. Cole, S.P. Multidrug resistance protein 1 (MRP1, ABCC1), a "multitasking" ATP-binding cassette (ABC) transporter. *Journal of Biological Chemistry* **2014**, *289*, 30880-30888.
30. Johnson, Z.L.; Chen, J. Structural basis of substrate recognition by the multidrug resistance protein MRP1. *Cell* **2017**, *168*, 1075-1085.
31. Johnson, Z.L.; Chen, J. ATP binding enables substrate release from multidrug resistance protein 1. *Cell* **2018**, *172*, 81-89.
32. Wang, L.; Johnson, Z.L.; Wasserman, M.R.; Levring, J.; Chen, J.; Liu, S. Characterization of the kinetic cycle of an ABC transporter by single-molecule and cryo-EM analyses. *Elife* **2020**, *9*, e56451.
33. Loe, D.W.; Almquist, K.C.; Deeley, R.G.; Cole, S.P. Multidrug Resistance Protein (MRP)-mediated Transport of Leukotriene C4 and Chemotherapeutic Agents in Membrane Vesicles: DEMONSTRATION OF GLUTATHIONE-DEPENDENT VINCRISTINE TRANSPORT (∗). *Journal of Biological Chemistry* **1996**, *271*, 9675-9682.
34. Mao, Q.; Deeley, R.G.; Cole, S.P. Functional reconstitution of substrate transport by purified multidrug resistance protein MRP1 (ABCC1) in phospholipid vesicles. *Journal of Biological Chemistry* **2000**, *275*, 34166-34172.
35. Cole, S.P. Targeting multidrug resistance protein 1 (MRP1, ABCC1): past, present, and future. *Annual review of pharmacology and toxicology* **2014**, *54*, 95-117.
36. Allikmets, R.; Schriml, L.M.; Hutchinson, A.; Romano-Spica, V.; Dean, M. A human placenta-specific ATP-binding cassette gene (ABCP) on chromosome 4q22 that is involved in multidrug resistance. *Cancer research* **1998**, *58*, 5337-5339.

37. Miyake, K.; Mickley, L.; Litman, T.; Zhan, Z.; Robey, R.; Cristensen, B.; Brangi, M.; Greenberger, L.; Dean, M.; Fojo, T. Molecular cloning of cDNAs which are highly overexpressed in mitoxantrone-resistant cells: demonstration of homology to ABC transport genes. *Cancer research* **1999**, *59*, 8-13.
38. Dean, M.; Hamon, Y.; Chimini, G. The human ATP-binding cassette (ABC) transporter superfamily. *Journal of lipid research* **2001**, *42*, 1007-1017.
39. Robey, R.W.; Polgar, O.; Deeken, J.; To, K.W.; Bates, S.E. ABCG2: determining its relevance in clinical drug resistance. *Cancer and Metastasis Reviews* **2007**, *26*, 39-57.
40. Mao, Q.; Unadkat, J.D. Role of the breast cancer resistance protein (BCRP/ABCG2) in drug transport—an update. *The AAPS journal* **2015**, *17*, 65-82.
41. Dezi, M.; Fribourg, P.-F.; Di Cicco, A.; Arnaud, O.; Marco, S.; Falson, P.; Di Pietro, A.; Lévy, D. The multidrug resistance half-transporter ABCG2 is purified as a tetramer upon selective extraction from membranes. *Biochimica et Biophysica Acta (BBA)-Biomembranes* **2010**, *1798*, 2094-2101.
42. McDevitt, C.A.; Collins, R.F.; Conway, M.; Modok, S.; Storm, J.; Kerr, I.D.; Ford, R.C.; Callaghan, R. Purification and 3D structural analysis of oligomeric human multidrug transporter ABCG2. *Structure* **2006**, *14*, 1623-1632.
43. Xu, J.; Liu, Y.; Yang, Y.; Bates, S.; Zhang, J. Characterization of oligomeric human half ABC transporter ABCG2/BCRP/MXR/ABCP in plasma membranes. *J Biol Chem* **2004**, *279*, 19781-19789.
44. Taylor, N.M.; Manolaridis, I.; Jackson, S.M.; Kowal, J.; Stahlberg, H.; Locher, K.P. Structure of the human multidrug transporter ABCG2. *Nature* **2017**, *546*, 504-509.
45. Jackson, S.M.; Manolaridis, I.; Kowal, J.; Zechner, M.; Taylor, N.M.; Bause, M.; Bauer, S.; Bartholomaeus, R.; Bernhardt, G.; Koenig, B. Structural basis of small-molecule inhibition of human multidrug transporter ABCG2. *Nature structural & molecular biology* **2018**, *25*, 333-340.
46. Manolaridis, I.; Jackson, S.M.; Taylor, N.M.; Kowal, J.; Stahlberg, H.; Locher, K.P. Cryo-EM structures of a human ABCG2 mutant trapped in ATP-bound and substrate-bound states. *Nature* **2018**, *563*, 426-430.
47. Orlando, B.J.; Liao, M. ABCG2 transports anticancer drugs via a closed-to-open switch. *Nature communications* **2020**, *11*, 1-11.
48. Kowal, J.; Ni, D.; Jackson, S.M.; Manolaridis, I.; Stahlberg, H.; Locher, K.P. Structural basis of drug recognition by the multidrug transporter ABCG2. *Journal of Molecular Biology* **2021**, *433*, 166980.
49. Yu, Q.; Ni, D.; Kowal, J.; Manolaridis, I.; Jackson, S.M.; Stahlberg, H.; Locher, K.P. Structures of ABCG2 under turnover conditions reveal a key step in the drug transport mechanism. *Nature Communications* **2021**, *12*, 1-12.
50. Allen, J.D.; Van Loevezijn, A.; Lakhai, J.M.; Van Der Valk, M.; Van Tellingen, O.; Reid, G.; Schellens, J.H.; Koomen, G.-J.; Schinkel, A.H. Potent and specific inhibition of the breast cancer resistance protein multidrug transporter in vitro and in mouse intestine by a novel analogue of fumitremorgin C. *Molecular cancer therapeutics* **2002**, *1*, 417-425.
51. Puentes, C.O.; Höcherl, P.; Kühnle, M.; Bauer, S.; Bürger, K.; Bernhardt, G.; Buschauer, A.; König, B. Solid phase synthesis of tariquidar-related modulators of ABC transporters preferring breast cancer resistance protein (ABCG2). *Bioorganic & medicinal chemistry letters* **2011**, *21*, 3654-3657.
52. Burger, H.; van Tol, H.; Boersma, A.W.; Brok, M.; Wiemer, E.A.; Stoter, G.; Nooter, K. Imatinib mesylate (STI571) is a substrate for the breast cancer resistance protein (BCRP)/ABCG2 drug pump. *Blood* **2004**, *104*, 2940-2942.
53. Eadie, L.; Hughes, T.; White, D. Interaction of the efflux transporters ABCB1 and ABCG2 with imatinib, nilotinib, and dasatinib. *Clinical Pharmacology & Therapeutics* **2014**, *95*, 294-306.
54. Houghton, P.J.; Germain, G.S.; Harwood, F.C.; Schuetz, J.D.; Stewart, C.F.; Buchdunger, E.; Traxler, P. Imatinib mesylate is a potent inhibitor of the ABCG2 (BCRP) transporter and reverses resistance to topotecan and SN-38 in vitro. *Cancer research* **2004**, *64*, 2333-2337.
55. Özvegy-Laczka, C.; Köblös, G.; Sarkadi, B.; Váradi, A. Single amino acid (482) variants of the ABCG2 multidrug transporter: major differences in transport capacity and substrate recognition. *Biochimica et Biophysica Acta (BBA)-Biomembranes* **2005**, *1668*, 53-63.
56. David, A.; Islam, S.; Tankhilevich, E.; Sternberg, M.J. The AlphaFold Database of Protein Structures: A Biologist's Guide. *Journal of Molecular Biology* **2022**, *434*, 167336.
57. Berthold, M.R.; Cebron, N.; Dill, F.; Gabriel, T.R.; Kötter, T.; Meinl, T.; Ohl, P.; Thiel, K.; Wiswedel, B. KNIME-the Konstanz information miner: version 2.0 and beyond. *AcM SIGKDD explorations Newsletter* **2009**, *11*, 26-31.
58. Jumper, J.; Evans, R.; Pritzel, A.; Green, T.; Figurnov, M.; Ronneberger, O.; Tunyasuvunakool, K.; Bates, R.; Žídek, A.; Potapenko, A. Highly accurate protein structure prediction with AlphaFold. *Nature* **2021**, *596*, 583-589.
59. Hrycyna, C.A.; Airan, L.E.; Germann, U.A.; Ambudkar, S.V.; Pastan, I.; Gottesman, M.M. Structural flexibility of the linker region of human P-glycoprotein permits ATP hydrolysis and drug transport. *Biochemistry* **1998**, *37*, 13660-13673.
60. Sato, T.; Kodan, A.; Kimura, Y.; Ueda, K.; Nakatsu, T.; Kato, H. Functional role of the linker region in purified human P-glycoprotein. *The FEBS journal* **2009**, *276*, 3504-3516.
61. Ferreira, R.J.; Ferreira, M.-J.U.; Dos Santos, D.J. Insights on P-glycoprotein's efflux mechanism obtained by molecular dynamics simulations. *Journal of Chemical Theory and Computation* **2012**, *8*, 1853-1864.
62. Ferreira, R.J.; Ferreira, M.J.U.; Dos Santos, D.J. Assessing the Stabilization of P-Glycoprotein's Nucleotide-Binding Domains by the Linker, Using Molecular Dynamics. *Molecular informatics* **2013**, *32*, 529-540.
63. Bonito, C.A.; Ferreira, R.J.; Ferreira, M.-J.U.; Gillet, J.-P.; Cordeiro, M.N.D.; Dos Santos, D.J. Theoretical insights on helix repacking as the origin of P-glycoprotein promiscuity. *Scientific reports* **2020**, *10*, 1-13.
64. ULC, C. Molecular Operating Environment (MOE), 1010 Sherbooke St. *West, Suite* **2017**, *910*.

 doi:10.20944/preprints202210.0066.v1

65. Ruff, K.M.; Pappu, R.V. AlphaFold and implications for intrinsically disordered proteins. *Journal of Molecular Biology* **2021**, 167208.
66. Kage, K.; Tsukahara, S.; Sugiyama, T.; Asada, S.; Ishikawa, E.; Tsuruo, T.; Sugimoto, Y. Dominant-negative inhibition of breast cancer resistance protein as drug efflux pump through the inhibition of S-S dependent homodimerization. *International journal of cancer* **2002**, *97*, 626-630.
67. Litman, T.; Jensen, U.; Hansen, A.; Covitz, K.-M.; Zhan, Z.; Fetsch, P.; Abati, A.; Hansen, P.R.; Horn, T.; Skovsgaard, T. Use of peptide antibodies to probe for the mitoxantrone resistance-associated protein MXR/BCRP/ABCP/ABCG2. *Biochimica et Biophysica Acta (BBA)-Biomembranes* **2002**, *1565*, 6-16.
68. Xu, J.; Liu, Y.; Yang, Y.; Bates, S.; Zhang, J.-T. Characterization of oligomeric human half-ABC transporter ATP-binding cassette G2. *Journal of Biological Chemistry* **2004**, *279*, 19781-19789.
69. László, L.; Sarkadi, B.; Hegedűs, T. Jump into a new fold—A homology based model for the ABCG2/BCRP multidrug transporter. *PLoS One* **2016**, *11*, e0164426.
70. Liu, Y.; Yang, Y.; Qi, J.; Peng, H.; Zhang, J.-T. Effect of cysteine mutagenesis on the function and disulfide bond formation of human ABCG2. *Journal of Pharmacology and Experimental Therapeutics* **2008**, *326*, 33-40.
71. Walzthoeni, T.; Leitner, A.; Stengel, F.; Aebersold, R. Mass spectrometry supported determination of protein complex structure. *Current opinion in structural biology* **2013**, *23*, 252-260.
72. Rossmann, M.G. Molecular replacement–historical background. *Acta Crystallographica Section D: Biological Crystallography* **2001**, *57*, 1360-1366.